Eur. Phys. J. D **39**, 199–208 (2006)
DOI: 10.1140/epjd/e2006-00094-2

THE EUROPEAN PHYSICAL JOURNAL D

Interaction of a supersonic beam of toluene with a resonant RF electric field

Observation of a strong beam splitting

M. Morato, J.O. Caceres, and A. González Ureña[a]

Instituto Pluridisciplinar, Unidad de Láseres y Haces Moleculares, Universidad Complutense de Madrid, Madrid-28040, Spain

Received 3 October 2005 / Received in final form 6 February 2006
Published online 28 April 2006

Abstract. Deflection of a cold supersonic toluene beam seeded in He has been observed when these molecules interact with both a static and a resonant oscillating electric field. The toluene beam splits into two beams each one peaking at a deflection angle of 1 degree towards the positive and negative direction of the Stark field when the employed resonant frequency between the two Stark levels of the toluene molecule is 1411 kHz. This deflection angle is about four orders of magnitude higher than the value one would expect from the toluene dipole moment and the employed RF field gradient. Different hypothesis are suggested to explain the observed strong beam splitting including the possibility of transverse beam interferences induced by both the resonant RF field and the transverse uniform electric field. A theoretical model is presented based on molecular beam interferences induced by the resonant RF field which seems to account satisfactorily for the present observations.

PACS. 32.60.+i Zeeman and Stark effects

1 Introduction

In series of previous papers our group has reported beam depletion spectra [1,2] of a NO supersonic beam when the polar NO molecules interact with a resonant RF field. In these experiments an anomalous first order Stark effect was observed [2] whose molecular explanation still remains open. More specifically in our previous study described in reference [1] strong beam deflection of a supersonic NO beam was observed when these polar molecules interact with both a static and a resonant oscillating electric field. A clear explanation of such beam deflection has not yet emerged. This new finding motivates the present investigation which was carried out using the same experimental technique used in reference [1] but with a different molecule, toluene which shows a clear linear Stark effect as described below.

In the present work we have investigated the interaction of a molecular beam of toluene with both a static and a resonant RF electric field. The molecular beam of toluene has been selected for various reasons. Toluene spectroscopy is well-known [3,4] and presents a resonant absorption at the fourth harmonic of the Nd:YAG laser (λ_{er} = 266 nm). This aromatic molecule can be easily ionised using low energy nanoseconds laser pulses. On the other hand the torsional motion of the CH_3 group [4], confers to the molecule a symmetric top character which can be accessed by first order Stark effect. In fact for the present investigation we have used the first order Stark effect for the $J = K = 1$ state (see below).

Our goal to carry out the present study was to understand the main reason for the observed beam depletion when polar molecules interact with resonant RF fields. We anticipate that a strong beam splitting was observed for the toluene supersonic beam when these molecules interact resonantly with the RF field. This new phenomenon seems to be due to beam interferences induced by both the resonant RF field and the transverse uniform electric field. A theoretical model is presented based on molecular beam interferences induced by the resonant RF field which seems to account satisfactorily for the present observations. The present results may open the way to new applications in the manipulation of matter as well as new studies in molecular interferometry.

2 Experimental and electric fieds' characteriztion

The main features of the molecular beam apparatus have been extensively described elsewhere [1,5] and only a brief description is given here. The present experiment employs a supersonic beam of toluene produced by bubbling 2 bar

[a] e-mail: laseres@pluri.ucm.es

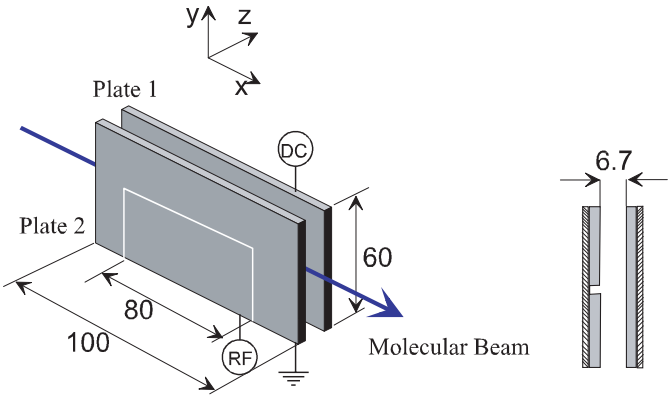

Fig. 1. Schematic view of the resonant unit: (left) perspective view including the DC and RF field connections. (Right) Front view in the yz-plane. All dimensions in mm.

of He though liquid toluene at 0 °C. The volatile impurities were removed from the toluene through freeze and thaw cycles.

The resonance unit is of the same type that described earlier [2,6]. Essentially it consists of two parallel Cu coated glass plates (length 10 cm along the beam, height 6 cm) separated by 0.67 cm. In one plate a 1 mm wide scratch insulates electrically a rectangle of 8 cm by 3 cm; the rectangle and the rest of the plate form the electrodes to which the RF is applied. The static voltage is applied to the rectangular electrode and the opposite plate. A schematic view of the resonant unit is shown in Figure 1 where a perspective view and a cut through the yz-plane are displayed. The collimated molecular beam is along the x-direction. As the molecule travels inside the RF unit it sees the static DC field along the z-direction and a perpendicular E_y field due to the oscillating RF field. The latter is time dependent and can be represented by the simple form

$$E_{RF} = E_0 \cos \omega t. \quad (1)$$

Here E_0 is the field amplitude, which is also z dependent. A numerical calculation of the E_y function, using the Simion 7.0 program, is illustrated in Figure 2a when the voltage of the lower RF plate is +15 V or –15 V and the upper panel is 0 V. In all cases the DC field is +10 V. Thus the RF field is perpendicular to both the molecular beam direction as well as to the static field direction. Furthermore it can be shown that the z dependence of the E_y field can be approximated by a function of the form $E_y = E_y(z = 0) + zE'_y$ where, for the present conditions, see Figure 2b, $E_y(z = 0) = 1.12$ kV/m and $E'_y = -610$ kV/m^2.

Besides the y-component of the RF field there is also a x-component at both sides of the resonant unit. For a better illustration of this effect, Figure 3 displays the E_x component over the length of the unit. In the Figure the two cases for which the RF field amplitude is ±15 V, are displayed. Obviously the E_z contribution due to the DC field is constant, $E_z = 1.49$ kV/m, i.e. it has no z dependence as $dE/dz = 0$. Of relevance for the present work is the x dependence of E_y component of the RF field.

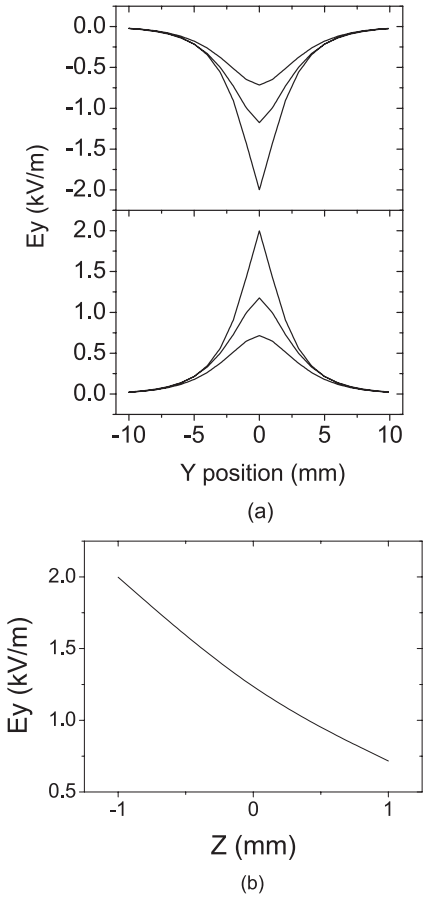

Fig. 2. (a) E_y values as a function of y. The following voltages were used: DC + 10 V. RF: top panel +15 V, bottom panel: –15 V. In both panels the central line corresponds to $z = 0$, i.e. right at the middle position between both plates. The upper line corresponds to $z = -1$ and +1 mm for the top and bottom panel, respectively. The bottom line for $z = +1$ and –1 mm, respectively. (b) E_y versus z for $y = 0$. The calculation was made when RF plate is at +15 V.

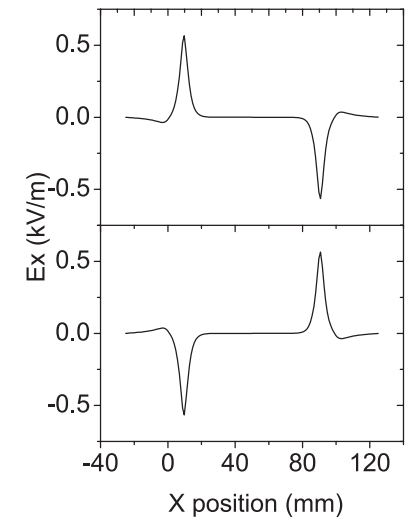

Fig. 3. E_x as a function of x for the same DC and RF values used in Figure 2. Top and bottom panel corresponds to RF plate +15 V and –15 V, respectively.

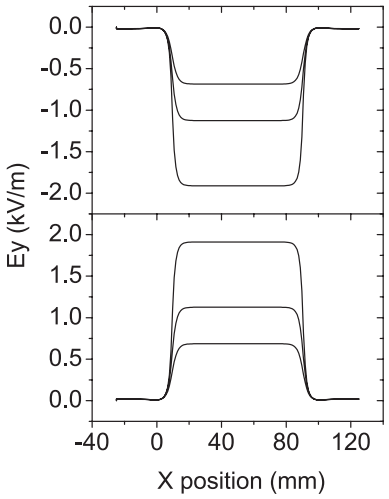

Fig. 4. Same presentation as in Figures 3 and 2 but for E_y.

It is shown in Figure 4 for the same two cases of +15 V and –15 V amplitude. Again the figure indicate the presence of a time dependent field over the x beam propagation. We can then summarize that as the molecule travels through the electric fields it experiences the following interactions:

(i) at the borders of the unit with first a small E_x gradient due to the side effects of the static field and, secondly, a time dependent E_x gradient due to the Radiofrequency field;
(ii) inside the electric unit with two types of fields. Namely: the E_z field due to the static DC field and the time dependent oscillating RF electric field. While the former has zero gradient $dE/dz = 0$ the latter has a gradient in the z-direction which can be approximated by a linear function of the type mentioned above.

The molecular beam runs parallel to the scratch (along the x-axis) 0.335 cm away from the plate. A movable slit was used to record the beam profile. The slit position can be changed by a computer controlled step motor by increments of 0.01 cm along the z-axis (i.e. perpendicular to the beam direction).

Two kinds of measurements were carried out. In the first one, depletion spectra are measured, when the slit position remains fixed at the centre of the molecular beam. In this case we want to emphasize that the measured signal consists of the toluene beam intensity after it passes the resonant unit. Here the toluene molecules interact with both an external Stark field and an oscillating electric field. The measured spectra consist of toluene beam intensity as a function of the frequency of the oscillation field for a fixed Stark field. In the second type of experiments, all experimental parameters, i.e. Stark, RF field and radiofrequency were fixed and only the slit position was changed. Thus the toluene signal intensity can be monitored as a function of the slit position to measure a deflection spectrum.

3 Theoretical model for molecular beam interferences

3.1 The molecular interferometer

To explore the possibility of beam interferences we have developed a theoretical model based on molecular interferences induced by the resonant RF field. In the following a brief description of the model is presented. The reader is addressed to reference [7] for more details.

The resonant unit made by the static DC field and the resonant RF field can be considered as a closed two-arm interferometer [8] of Ramsey type in which the two radio-frequency zones, located at the entrance and exit of the unit, act as beam dividers. In these regions the RF fields induce transitions among the Stark levels split by the DC field as in a classic Ramsey separated oscillatory fields set-up. In between the beam dividers the 'phase object' [8] consists of the time-dependent electric field profile depicted in Figure 2. While the first RF fields creates a coherent superposition of the two (J.M) Stark sub-levels, the second region re-superposes the outgoing wave before the molecular beam is detected. The phase object of the interferometer is the RF field created by the horizontal scratch along the beam propagation direction. This field creates under resonant conditions a distinct interaction potential on the different arms, i.e. on the distinct M_1 and M_2 states and consequently, a phase shift is introduced between these two states. As a result the interference is frozen and its pattern is observed by scanning the phase difference accumulated in between the two separated RF field dividers. In the present work the latter is done both by changing the frequency of the RF field or in some other cases probing the transverse beam profile by a movable slit located in front of the detector, see below.

3.2 The phase shift

In our experiments the potential variation due to Stark interaction is always equal or below 1 MHz ($\sim 10^{-9}$ eV) which is less than the molecule kinetic energy in our case $\sim$0.1 eV. Thus, the external motion of the molecule can be considered as uniform and the only action of the potential is restricted to an action on the internal (M) component part of the wavefunction. In other words, the main consequence to be expected of the electrostatic potential is the change for each M component. Therefore the phase shift $\phi_{M'}$ can be simplified by $\phi_M = M\phi$ where the phase shifts for $M = 1$, ϕ is given by the Glauber formalism [9] as:

$$\phi = -\frac{1}{\hbar\nu}\int_0^L W_{stark}\, dx. \qquad (2)$$

Here W_{stark} is the Stark energy for $M = 1$ and ν is the particle velocity along the beam propagation (x-axis) direction and L the length of the resonant unit. When the oscillating RF field is turned on a time dependent field, given by $E_{RF} = E_0 \cos\omega t$, may interact with the dipole

moment and under resonant conditions interferences may be possible.

As mentioned earlier the resonant RF field induces a coherent superposition between the two M states involved in the transition, these two states are therefore the different arms of our two-arm interferometer [8]. Since the interaction energy W_{RF} is much smaller than the initial kinetic energy it only induces an extra phase shift between the two states $\delta\phi$ given by [8]:

$$\delta\phi = \phi_{M_1} - \phi_{M_2} \tag{3}$$

being M_1 and M_2 the two Stark levels coupled by the RF field. Since in our experiment a perpendicular transition is used i.e. $|\Delta M| = 1$ the extra phase shift $\delta\phi$ reduces to ϕ which is given by equation (2).

The interaction of a two-level system with a static and an oscillating RF field is a well-known model system in quantum mechanics. The first order perturbation treatment was developed by Rabi with standard formulae [10] for a non degenerate two–level system interacting with an electromagnetic field E via an electric–dipole moment [10]. The interaction Hamiltonian can be written as

$$H(t) = -\mu_{12} E \cos\omega t \tag{4}$$

where μ_{12} is the transition dipole moment and ω the angular frequency of the radiation $E_1 = \hbar\omega_1$ is the energy of the lower state and $E_2 = \hbar\omega_2$ that of the upper state. Thus the energy difference is $\Delta E = \hbar\omega_0 = \hbar(\omega_2 - \omega_1)$ with ω_0 the resonant frequency for transition between two states. For the present work we have adopted a simple model in which the dipole moment has the x and y component given by

$$\mu_y = \mu_{12}\cos\omega_0 t \tag{5a}$$

$$\mu_x = \mu_{12}\sin\omega_0 t \tag{5b}$$

i.e. it is rotating with the resonant frequency, ω_0. in the xy-plane. This model is a good approximation for near resonant conditions. To calculate the phase shift accumulation due to this dipole moment interaction with the RF field we use the model potential depicted in Figure 4. Here the oscillating E_y field is given by $E_0\cos\omega t$. Thus the W_{RF} interaction energy adopts the form:

$$\begin{aligned} W_{RF} &= -\mu_{12}E_0\cos\omega_0 t\cos\omega t \\ &= -\mu_{12}E_0\frac{1}{2}\{\cos(\omega_0-\omega)t + \cos(\omega_0+\omega)t\}. \end{aligned} \tag{6}$$

Substituting this value in the phase shift equation one gets:

$$\begin{aligned} \phi = -\frac{1}{\hbar\nu}\left(-\mu_{12}E_0\right) \\ \times\frac{1}{2}\int_0^L \{\cos\left(\omega_0-\omega\right)t + \cos\left(\omega_0+\omega\right)t\}\,dx. \end{aligned} \tag{7}$$

Replacing x by t, i.e. we uses $x = \nu t$, one obtains

$$\phi = \frac{1}{2}\omega_1\int_0^T (\cos(\omega_0-\omega)t + \cos(\omega_0+\omega)t)dt \tag{8}$$

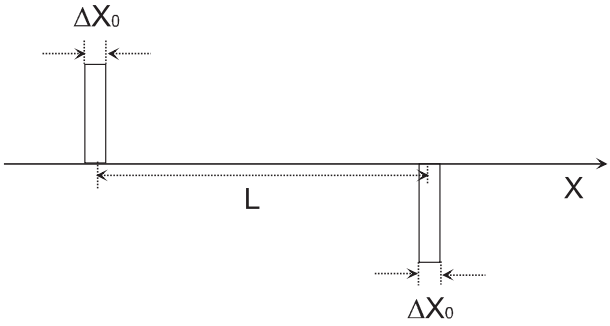

Fig. 5. Model potential to simulate the edge effects: two opposite rectangular field profiles are located at the entrance and exit channels of the resonant unit.

where ω_1 is the Rabi frequency $\omega_1 = \mu_{12}E_0/\hbar$ and $T = L/\nu$.

Integration from 0 to T leads to the result

$$\phi = \frac{1}{2}\omega_1 T\left[\frac{\sin\left(\omega_0-\omega\right)T}{\left(\omega_0-\omega\right)T} + \frac{\sin\left(\omega_0+\omega\right)T}{\left(\omega_0+\omega\right)T}\right]. \tag{9}$$

For frequencies such that $(\omega_0+\omega)\,T \gg 1$ the second term can be neglected and the phase shift reduces to

$$\phi \approx \frac{1}{2}\omega_1 T\frac{\sin\left(\omega_0-\omega\right)T}{\left(\omega_0-\omega\right)T}. \tag{10}$$

Thus, when $\omega \to \omega_0$,

$$\frac{\sin\left(\omega_0-\omega\right)T}{\left(\omega_0-\omega\right)T} \to 1 \quad \text{and} \quad \phi_0 = \frac{1}{2}\omega_1 T. \tag{11}$$

Furthermore, the phase shift shows an oscillatory behaviour with maxima at

$$(\omega_0-\omega)T = (2n-1)\frac{\pi}{2} \quad (n = 1, 2, 3...). \tag{12}$$

3.3 Effect of the edge potentials

As illustrated in Figure 3 there are opposite potentials at the border of the resonant unit. We have incorporated this edge effect by considering the model potential shown in Figure 5 in which Δx_0 is the length of the entrance and exit barrier which for the present set-up is few millimeters. Applying the same model and treatment of the previous section but now with the x component of the dipole moment one obtains a new contribution for the accumulated phase shift given by

$$\phi = \frac{1}{2}\frac{\omega_1}{\Delta\omega}\{-\sin\Delta\omega(T+\tau) + \sin\Delta\omega\tau + \sin\Delta\omega T\} \tag{13}$$

where $\Delta\omega = \omega_0 - \omega$ and τ is the time the molecule feels the perturbation of the entrance or exit barrier potentials. It is clear that at resonance $\Delta\omega$ and, therefore, the accumulated phase shift due to these edge effects is zero.

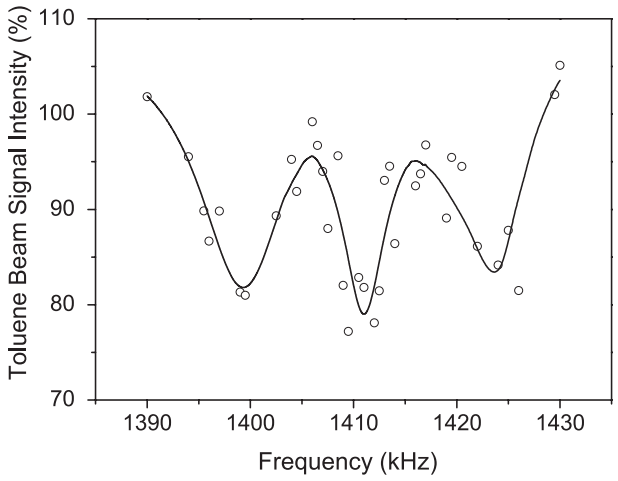

Fig. 6. Toluene beam depletion spectrum as function of the RF field frequency. Notice the dip resonance at 1411 kHz and the two sideband peaks. Open circles: experimental data. Solid line is just drawn to guide the eye. The data was taken at $E = 1.49$ kV/m and a RF peak-to-peak voltage of 30 V. Stagnation pressure was 2 bars. See text for comments.

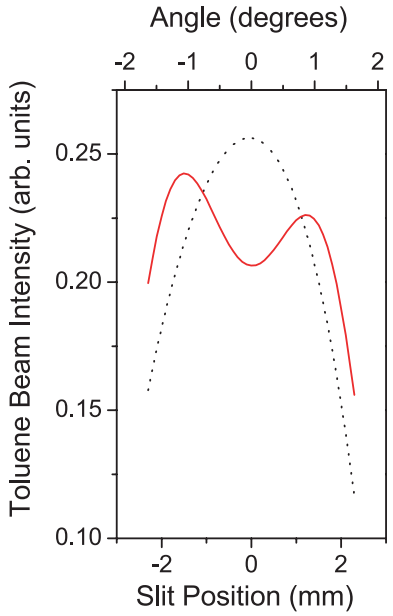

Fig. 7. Toluene signal intensity as a function of the slit position. Broken line refers to beam profile intensity measured under off resonant conditions ($\nu_{off} = 1300$ kHz) and solid line refers to the same type of measurement taken at resonant conditions ($\nu_{on} = 1411$ kHz). Notice the splitting towards both $\pm z$-directions when the beam interacts with the resonant RF field. The DC and RF field strengths were the same as those used in Figure 6.

3.4 Total beam signal

To estimate the beam signal at the detector we consider a single molecule resonantly interacting with the RF field. In this case, the measured signal results from the average of a single molecule squared wavefunction over all statically distributed parameter like velocity, angle distribution, etc. It can be shown that for the simple two arms interferometer [8], the single molecule signal, S, has the form

$$S = \langle \Psi / \Psi \rangle = C + D\cos(\delta\phi) = C + D\cos\phi \qquad (14)$$

where C and D are coefficients characteristic of the pair of beam dividers. Thus under the constraints of the present model the average signal should be the convolution of S over the size of the collimator in front of the defector and the velocity beam distribution. The first convolution is simply given by

$$S = \int_0^R (C + D\cos\phi) 2\pi z dz. \qquad (15)$$

In which where we have assumed a circular collimator of radius R. The simplest model interaction is to assume that the phase shift does not depend on the transversal axis and therefore the average (single-velocity) signal intensity is:

$$\langle S \rangle = \pi R^2 (C + D\cos\phi) = \pi R^2 [C + D\cos\phi]. \qquad (16)$$

Far from resonance $\phi = 0$ and $S(\infty) = \pi R^2 (C + D)$. At resonant conditions $S(\omega_0) = \pi R^2 (C + D\cos\phi_0)$. We can then define the normalised signal S^* as

$$S^* = \frac{S(\infty) - S(\omega)}{S(\infty) - S(\omega_0)} \qquad (17)$$

which is given by

$$S^* = \frac{1 - \cos\phi}{1 - \cos\phi_0} \qquad (18)$$

here ϕ_0 is the extra phase shift at resonant conditions.

4 Results

The transmitted toluene signal vs. the oscillating frequency for a DC field strength, E, of 1.49 kV/m and a R.F. field strength, E_0, of 1.12 kV/m with the slit allocated at the centre of the molecular beam is shown in Figure 6. A clear dip at 1411 kHz and about 22% attenuation is observed. Two sideband peaks of a similar intensity also appear around ± 12 kHz of the central dip frequency. Interestingly the frequency of the central dip is the expected resonant frequency according to equation (22) below.

Figure 7 shows the second type of measurement taken in the present investigation. The beam signal intensity is displayed as a function of the slit position. Two beam profiles are displayed at two distinct RF frequencies; 1411 kHz (on resonance) and 1300 kHz (off resonance). Sixty laser shoots were averaged for each slit position, which was moved by 0.01 cm increments. To reduce possible effects due to signal drifts, one ON beam profile measurement was followed by one OFF beam profile measurement and so on.

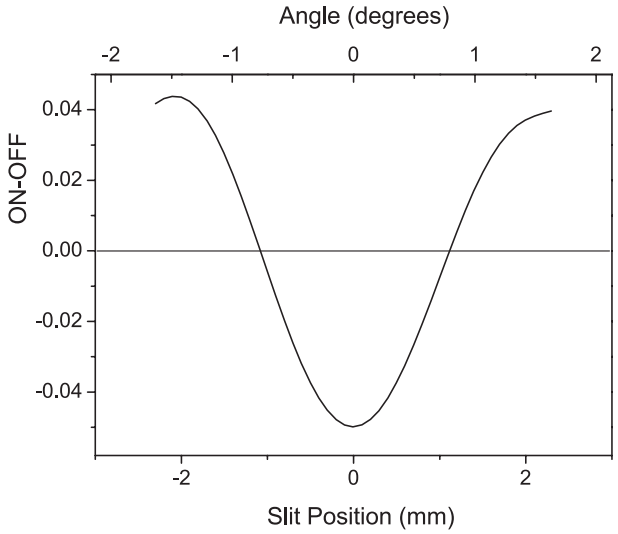

Fig. 8. Variation of the toluene beam intensity as a function of the slit position. At each position the (ON-OFF) beam signal is plotted. ON and OFF stand for the toluene signal measured at 1411 kHz and 1300 kHz conditions, respectively.

As shown in the figure the beam splits into two beams at resonant conditions. Each split beam peaks at 1 degree taking the centre of the resonant unit as the origin for the beam deflection. Interestingly, the total beam signal, i.e. the signal integral over the slit position is, within the experimental error, the same for the two beam profiles. The latter indicates that the main difference between the two measurements is the beam splitting towards the negative and positive direction of the z-axis. Hence this beam deflection leads to signal depletion when one monitors the beam intensity with a fixed slit and detector located at the centre of the collimated beam.

For a better illustration of both the extent and direction of the beam deflection Figure 8 displays the (ON-OFF) beam signal. Here ON and OFF refer to the measured beam signal at 1411 kHz and 1300 kHz conditions, respectively. In this plot the beam deflection towards the $\pm z$-direction is clearly noticed.

Looking at the profiles several points are important to be remarked. First of all the significant deflection, which is about 1 degree. Secondly, it is interesting to notice the symmetric character of the deflexion. Due to the action of the resonant field the profile moves to the right and left direction, i.e. the molecules affected by the resonant interaction are deflected towards the $\pm z$-directions.

5 Discussion

5.1 Stark interaction

When a molecule with a permanent electric dipole moment, μ, interacts with a homogeneous static Stark field, with E as field strength the energy of the molecule is perturbed and given by [10–13]

$$W = W_0 + W_{Stark} \tag{19}$$

in which W_0 is the energy of the unperturbed system (i.e. when $E = 0$) and $W_{Stark} = -\overline{\mu}_E E$. Here $\overline{\mu}_E$ is the mean component of the electric moment in the field direction. If the linear molecule is in a Σ state the dipole moment is perpendicular to the total angular momentum (we neglect spin effects) and therefore $\overline{\mu}_E = 0$. In other works, there is no first order Stark splitting [10]. However, there is a second order effect when one considers the action of the Stark field on the molecular rotation.

For a symmetric top molecule $\overline{\mu}_E$ is not longer zero and a linear Stark effect arises given by [12,13]

$$W_{stark} = -\mu E \frac{KM}{J(J+1)}. \tag{20}$$

Here μ is the permanent electric dipole moment which in the case of the toluene molecule equals $\mu = 0.375$ D [14], J the total angular momentum, K the magnitude of the projection of J on the top axis and M the projection of J on the space fixed axis, i.e. the direction of the static E field. In this work we restrict ourselves to the K= 1 case. Consequently, the Stark interaction is given by

$$W_{stark(k=1)} = -\mu E \frac{M}{J(J+1)}. \tag{21}$$

Thus, the $\Delta M = \pm 1$ transition corresponds to an energy splitting of:

$$\Delta W_{stark} = h\nu_0 = \mu E/(J(J+1)). \tag{22}$$

Inserting $J = 1$ and $\Delta M = 1$ one obtains the resonant frequencies $\nu_0 = \mu E/2h$, which for $E = 1.49$ kV/m gives 1411 kHz. This value exactly corresponds to the experimentally observed one, for the central dip of Figure 6, the sideband peaks cannot be justified by Rabi oscillations and they seem to be a consequence of Ramsey type interferences (see below).

5.2 Particle deflection

One crucial question also raised by the present results, is the mechanism for the beam deflection, i.e. the observed symmetric deflection of the order of ca. 1°. The splitting of the molecular beam into two beams towards the positive and negative z-directions can be rationalised by the transverse Stern-Gerlach deflection [15]. While in the classic Stern-Gerlach experiment the beam deflection is due to the gradient of the (static) non-homogeneous field in the present case it could be originated by the gradient of the resonant RF field.

A dipole $\overrightarrow{\mu}$ moving through an electric $\overrightarrow{E}(z,t)$ field has an interaction energy, W, given by

$$W = -\overrightarrow{\mu} \cdot \overrightarrow{E}(z,t) \tag{23}$$

if E is uniform in space such an interaction will have no effect on the spatial motion of the particle. However, if E depends on z a net force will act on the particle F_z and is given by

$$F_z = -\frac{\partial W}{\partial z} = \mu \frac{\partial E}{\partial z}. \quad (24)$$

This interaction will tend to cause the particle to move to regions of space that minimize the energy. For example if $\overrightarrow{\mu}$ is parallel to $\overrightarrow{E}$, W will be negative and consequently, the particle be forced toward regions of larger E so that W is even smaller (more negative). By contrast, if the moment is antiparallel to the field, W would be positive and the particle will then be forced toward regions of smaller E.

In our case the particle can be considered as asymmetric top and the effective dipole moment $\mu_{eff} = \mu\langle\cos\theta\rangle$. Here $\langle\cos\theta\rangle$ is the mean value of $\cos\theta$ where θ is the angle between μ and the electric field. The quantum mechanical value of $\langle\cos\theta\rangle$ is given by [13]:

$$\langle\cos\theta\rangle = \frac{KM}{J(J+1)}.$$

Thus the interaction energy is therefore that given by equation (20) and the force along the z-axis is

$$F_z = \mu \frac{KM}{J(J+1)} \frac{\delta E}{\delta z}. \quad (25)$$

In the conventional Stern-Gerlach experiment the three M states equally populated, would produce two equally split beams in addition to an undeflected central one.

For a simple two-level system with initial state populations given by N_1 and N_2, the time evolution of a given state population is controlled by the Rabi transition probability [10]. Obviously if the initial state population N_1 and N_2 is the same this equally populated distribution will not change with time as the probably P_{12} is equal to P_{21}. Even in case the initial state population was not statistical, after a very long time, i.e. after the action of a large number of Rabi cycles, the population would reach its statistical limit.

Under our experimental conditions the estimated Rabi frequency is about 750 kHz. Taking into account that the measured peak beam velocity is 500 m/s and the length of the RF unit 0.08 m one gets an average number of 754 Rabi cycles during the passage time through the resonant RF unit. The observation in Figure 2 that neither the deflected nor undeflected parts of the beam have the same intensity indicates that the transition probability given by the Rabi formula is not playing the main role in the observation here reported. In addition the magnitude of the deflection is surprisingly too large to be explained under the action of the RF field gradient. In other words, the beam deflection cannot be described by a type of transverse Stern-Gerlach experiment.

In fact deflection of a CsF beam by a resonant RF field has been observed by Hill and Gallager [16]. According to these authors a spatially inhomogeneous oscillating field tuned to the transition frequency between adjacent rotational states of a polar molecule exerts a force onto the molecule that leads to a resonance deflection. The force is due to the interaction of the oscillating field with the permanent dipole moment both of which rotates with the same frequency at resonance and is given by the negative gradient of the interaction energy. The authors studied a CsF beam and observed at a frequency resonant with the $J = 0$ and $J = 1$ transition of the vibrational and electronic ground state a significant deflection that can be fairly well described by this model. If applied to the present system it provides the largest force conceivable in the framework of electrostatic interaction $F < -\mu_z d/dz(E_1)$ where μ_z is the mean z-component of μ.

The maximal deflection angle is then given by $\theta_{max} = FL/(2E_{tr})$. With $L = 0.08$ m (the length of the interaction region), $E_{tr} = 0.12$ eV (the mean translational energy of toluene), $d/dz(E_0) = -610$ kV/m^2 and $\mu_z = \mu$ one obtains $\theta_{max} < 10^{-4}$ degrees, a value that is by orders of magnitude too small with respect to the observed one. Thus the RF gradient force acting on a free molecule cannot be responsible for the particle deflection. The observed deflection angle of ca. 1 degree would indicate a strong force acting on the toluene molecule considering its average beam velocity of 500 m/s and an average residence time (i.e. the molecule spends inside the resonant unit) of 160 μs.

Of relevance for the present observation of the toluene beam splitting is the possibility of an enhanced molecular orientation of the rotational distribution inside the cold beam by the combined action of a static and oscillating field and to whether it could be somehow responsible for the observed phenomenon. In this regard, Friedrich and Herschbach [17,18] have demonstrated the occurrence of a (pseudo) first order Stark effect for a polar molecule under the action of a non-resonant laser field combined with an even small static electric field. First the non-resonant strong laser pulse creates a significant alignment of the rotational angular momentum distribution. Subsequently, the action of a static electric field converts the rotational alignment distribution into an oriented distribution. The pendular hybridisation by the polarizability interaction has found several applications in spectroscopy and in focusing or aligning neutral molecules by means of an intense nanosecond laser pulse [18]. Furthermore, this new method to orient a polar molecule has been used in the study of the HXeI photofragmentation dynamics by Buck and co-workers [19,20].

Taking into consideration the combined action of the two fields one could think in the possibility to achieve molecular orientation by the combination of the rotational alignment originated by strong collisions in supersonic expansions followed by the action of a static electric field. Rotational alignment in supersonic expansions has been evidence by Aquilanti and co-workers [21]. Therefore it is not far from expectation to think that we may have an oriented toluene rotational distribution as a result of the combined action of the strong alignment during the supersonic expansion plus the action of the static and/or resonant RF field.

Even assuming that the rotational population of toluene molecules was significantly oriented by the combined action of both electric fields, it would be difficult to justify the observed strong beam splitting from such an oriented polar ensemble. The macroscopic total dipole moment, P, of such ensemble would be bound to an upper limit given by $P \leq N\mu$. Here N is the number of particles of the ensemble and μ the individual dipole moment. The maximum force acting on a molecule of the oriented ensemble due to the interaction with the electric field would not be higher than that of on a single isolated molecule with its individual moment given by μ. Hence there is no physical reason to expect that the deflection of the oriental molecular ensemble be higher than that of an isolated polar molecule.

5.3 Molecular beam interferences

A possibility to explain the strong beam splitting is the presence of interferences modulating the profile of the supersonic beam. Stern-Gerlach interferometric studies with atomic beams have shown interference patterns in the transverse plane of the beam. Indeed, Viaris de Lesegno et al. [22] have shown the possibility of modulating the transverse profile of a metastable argon beam by an interference pattern when a quadrupole magnetic field is incorporated at the heart of the interferometer. These authors also demonstrated that the addition of a homogeneous field allowed a translation of the pattern as a whole in any transverse direction. The Physics behind these interference patterns [22,23] is that a radial static magnetic field is used as a phase object inside a Stern-Gerlach atomic interferometer. This field produces phase shifts which are proportional to the distance to the zero-field line that is the atomic beam propagation axis. Thus, the transverse intensity profile of the atomic beam resulted modulated by an interference pattern that is exactly a "phase portrait" of the applied field configuration.

Figure 9 presents the comparison between the experimental transmission spectrum and the theoretically calculated one. The comparison is made using the normalised quantity S^* which ranges form zero (far from resonance) to 1 right at the central resonance dip. The simulated spectrum was obtained using equation (18) with the $\omega_0 = 1411$ kHz and the best fit value of $\omega_1 = 753.977$ kHz which is in very good agreement with the calculated Rabi frequency of 750 kHz. The agreement between both spectra is satisfactory. The model for molecular interferometer is capable to reproduce satisfactorily not only the central resonance dip but also the sideband structure of the transmitted spectrum. The relative intensity of the sidebands with respect to the central one is lower for the calculated spectrum than that of the experimental one. This maybe due to the simplicity of the model used here. For example, no consideration was given to the frequency dependence of the transition probability, which could have been taken into consideration by using a more complete treatment based on the Rabi transition probability. Nevertheless, the point to be remarked is the capability of our model to reproduce the main feature of the experimental depletion spectrum that is the depletion peak at the resonant frequency.

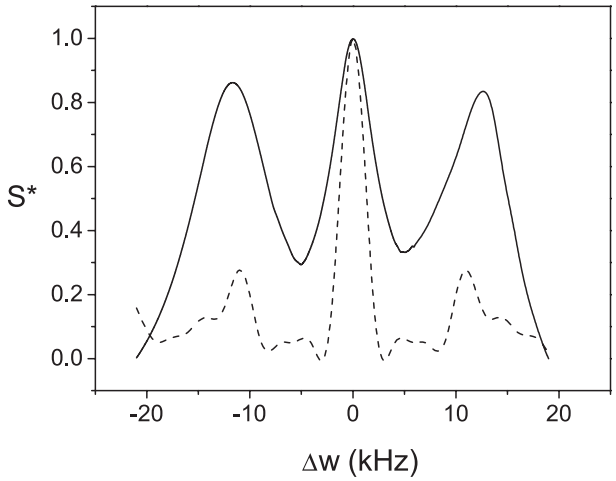

Fig. 9. Comparison between experimental and theoretical transmission spectra for the toluene beam as a function of the oscillating frequency of the RF field. The S^* values are used as follows. Solid line is the experimental S^* values estimated from the solid line of Figure 6 and using equation (18) of the text. Broken line calculated S^* values using equation (18) with $\omega_0 = 1411$ kHz and $\omega_1 = 753.977$ kHz. See text for comments.

5.4 Interferences in the transverse profile

Equation (18) contains a direct dependence of the beam profile on the z-axis providing that $\delta E\,(z,x)/\delta z \neq 0$, which is the present case.

Actually, the beam profile was calculated for a z-dependence of E_y given by (see Fig. 2b) $E_z = 1.12\ \mathrm{kV/m} - z \times 610\ \mathrm{kV/m}$ being z is in meters. Figure 10 displays both the calculated and experimental S^* values as a function of z. The calculation was done using equation (18) and the field gradient mentioned above. Both the velocity spread of the beam and the silt width were taken into account. Though the calculated splitting of the beam is lower than the experimentally found value, the angular locations of the split beams are closer to the experimental values The overall result is satisfactory taking into account the simplicity of the model and the moderate resolution of our experiment.

A more complete quantum treatment, that also will take into account the rotational population of the beam, is now in progress with the hope to reproduce more quantitatively the experimental spectra. Nevertheless, the point we would like to emphasize is the capability of the simple interference model to predict the beam splitting. Clearly, the gradient of the RF field along the transverse direction is responsible for the observed beam splitting (interference) in the beam profile.

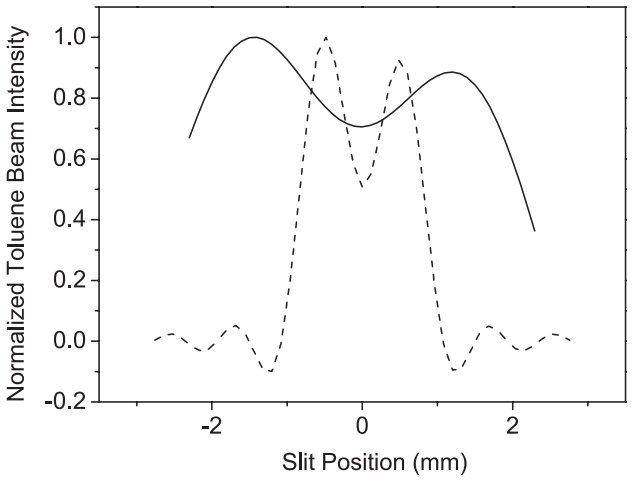

Fig. 10. Comparison between experimental and theoretical toluene beam profiles. Solid line experimental profile. It is the solid line from figure normalised to one at the peak Broken line calculated S^* values using equation (18) with $\omega_0 = 1411$ kHz and) $E_z = 1.12$ kV/m $- z \times 610$ kV/m. See text for comments.

6 Concluding remarks

In this work we have reported measurements on the toluene beam signal intensities recorded by Laser ionisation coupled with time-of-flight mass spectrometry. The beam signal was measured after the toluene molecules passed through a RF unit in which these molecules interact with both a static DC and oscillating RF electric fields. Essentially, two types of measurements were recorded (i) beam depletion spectra and (ii) beam profile signal. In the former the beam transmission signal is recorded as a function of the frequency of RF field for a fixed DC field. In the second case the beam profile is measured for a given DC and RF field values.

The main finding of the present investigation is the observation of a significant beam splitting when the molecular beam of toluene interacts with a resonant RF frequency between the two Stark levels split by the DC field. The beam splits into two beams each one deflected by 1° to both the positive and negative z-direction. The deflection is responsible for the beam depletion spectrum taken when the slit is fixed at the central beam position.

Of major relevance is the extent of the observed beam splitting. The measured deflection angle of 1 degree is several orders of magnitude higher than the calculated value based on the toluene dipole moment and the experimental RF field gradient. A theoretical model was presented based on molecular beam interferences, which seems to account for the main features of the observations. In this view, both the beam depletion and splitting seem to be due to beam interferences induced by both the resonant RF field and the uniform electric field.

It is remarkable to note that this simple resonant unit used in early molecular beam electric resonance studies [24] may act as a simple molecular interferometer of Ramsey type in which the two radio-frequency zones, located at the borders of the electric unit, act as beam dividers inducing transitions among the Stark levels split by the DC field. In between the beam dividers the 'phase object' consists of another RF electric field that introduces a phase shift between the two Stark sub-states. Thus, the resulting interferences are frozen and can be observed by scanning the phase difference accumulated in between the two beam dividers. In the present work two examples were shown: (i) in the total transmitted beam signal as a function of the RF frequency and (ii) in the transverse beam profile Despite the simplicity of the model it is capable to reproduce the main features of the observations i.e. the main peaks in the depletion spectrum and the main structure of the transverse beam profile. A more complete quantum treatment is being developed whose application will be the subject of a future paper.

To conclude we would like to emphasize the possibility to exploit the experimental set-up for new applications in the manipulation of matter and more specifically to carry out investigations in molecular interferometry.

Financial support from the Ministerial de Educación y Ciencia of Spain (grant CTQ2004–3468) is gratefully acknowledged. J.O. Caceres acknowledges a Ramón y Cajal Research Contract from The Ministerio de Educación y Ciencia of Spain. The authors thank Dr. Skowronek for his technical assistance in the design of the movable slit. The authors also thank the Comunidad de Madrid and the Universidad Complutense for a joint research grant.

References

1. M. Morato, J.O. Cáceres, A. González Ureña, Eur. Phys. J. D **38**, 215 (2006)
2. C. Montero, A. González Ureña, J.O. Caceres, M. Morato, J. Najera, H.J. Loesch, Eur. Phys. J. D **26**, 261 (2003)
3. D.R. Bursts, D.W. Pratl, J. Chem. Phys. **113**, 3658 (2000)
4. P.M. Brodersen, R.D. Gordon, J. Mol. Struct. **522**, 279 (2000)
5. K. Gasmi, A. Gonzalez Ureña, Chem. Phys. Lett. **410**, 82 (2005) and reference [1] cited therein
6. M. Morato, K. Gasmi, C. Montero, A. González Ureña, Chem. Phys. Lett. **392**, 255 (2004)
7. A. González Ureña et al., in preparation
8. J. Bandon, R. Mathevet, J. Robert, J. Phys. B: At. Mol. Opt. Phys. **32**, R173 (1999)
9. R.J. Glauber, *Lectures in theoretical physics* (Interscience, New-York, 1959), Vol. 1
10. N.F. Ramsey, *Molecular Beams* (Oxford University Press, Oxford, 1956); see also B.H. Bransder, C.J. Joachain, in *Physics of Atoms and Molecules* (Longman, London, 1983), p. 558
11. J.H. van Vleck, *The Theory of Electric and Magnetic Susceptibilities* (Oxford University Press, Oxford, 1932)
12. G. Herzberg, in *Molecular Spectra and Molecular Structure*, Vol. I, *Spectra of diatomic Molecules* (Van Nostrand Reinhold Company, New York, 1950), pp. 307–308

13. C.H. Townes, A.L. Schawlow, *Microwave Spectroscopy* (Dover Publications, Inc., New York, 1975)
14. *Handbook of Chemistry and Physics*, 74th edn. (Chemical Rubber Publishing Compagny, Ohio, USA, 1993–1994)
15. M. Bloom, E. Enga, Can. J. Phys. **45**, 1481 (1967)
16. R.M. Hill, T.F. Gallagher, Phys. Rev. A **12**, 451 (1975)
17. B. Friedrich, D. Herschbach, J. Chem. Phys. **111**, 6157 (1999)
18. B. Friedrich, D. Herschbach, J. Phys. Chem. A **103**, 10280 (1999)
19. N. Hendrik Nahler, R. Baumfalk, U. Buck, Z. Bihary, R.B. Gerber, B. Friedrich, J. Chem. Phys. **119**, 224 (2003)
20. N. Hendrik Nahler, M. Farnik, U. Buck, Chem. Phys. **301**, 173 (2004)
21. V. Aquilanti, D. Ascenzi, D. Cappelletti, F. Pirani, Nature **371**, 399 (1994)
22. B. Viaris de Lesegno, J.C. Karam, M. Boustimi, F. Perales, C. Mainos, J. Reinhardt, J. Baudon, V. Bocvarski, D. Grancharova, F. Pereira Dos Santos, T. Durt, H. Haberland, J. Robert, Eur. Phys. J. D **23**, 25 (2003)
23. M. Boustimi, V. Bocvarski, B. Viaris de Lesegno, K. Brodsky, F. Perales, J. Baudon, J. Robert, Phys. Rev. A **61**, 033602 (2000)
24. J.W. Trischka, Phys. Rev. **74**, 718 (1948)